

EFFECT OF ELECTRON-MAGNON INTERACTION ON THE Ni^{2+} ABSORPTION BAND IN MAGNETICALLY ORDERED CRYSTALS

A. I. BELYAEVA and V. V. EREMENKO

Physico-technical Institute of Low Temperatures, Academy of Sciences, Ukrainian S.S.R.

Submitted November 14, 1967

Zh. Eksp. Teor. Fiz. 54, 1303-1309 (May, 1968)

The fine structure of the ${}^3A_{2g} \rightarrow {}^1T_{2g}^a$ and ${}^3A_{2g} \rightarrow {}^3T_{1g}^b$ transitions in the Ni^{2+} -containing compounds KNiF_3 , K_2NiF_4 , RbNiF_3 , and NiF_2 possessing different crystallographic and magnetic structures is studied in detail. The temperature was varied between 1.3° and 77°K . At low temperatures ($T \ll T_N$), a T^4 dependence of the line shifts and broadening is found for all the no-magnon absorption bands; this is consistent with the theory in^[6,16]. The observed unique correspondence between the shift and broadening for no-magnon bands also agrees with^[16]. The nonlinear relation between the shift and broadening for the $\nu = 20\,622\text{ cm}^{-1}$ band in NiF_2 is interpreted as an additional proof of its electron-magnon nature.

THE effect of magnetic ordering on the positions and widths of 3d optical absorption bands in antiferromagnetic dielectrics has been determined experimentally.^[1-4] Attempts have been made to obtain a theoretical explanation of this effect at low temperatures $T \ll T_N$ (the Néel temperature). In^[5] a study was made of the broadening and shifts of pure electronic transition lines, resulting from an interaction between absorption-center electrons and spin waves in ferromagnets and antiferromagnets. Similar questions have been discussed for exciton transitions.^[6] However the theories could not be tested, mainly because the experimental data at $T \ll T_N$ were not very accurate as a result of the wide absorption bands representing transitions in the unfilled 3d shell of a transition metal ion, even at low temperatures. We have therefore investigated the temperature dependence of the widths and spectral positions of the narrowest Ni^{2+} absorption bands in magnetically ordered crystals.

Our experimental samples were four compounds containing Ni^{2+} , with different crystallographic and magnetic structures; these were collinear antiferromagnets (KNiF_3 and K_2NiF_4), a ferrimagnet (RbNiF_3), and a weakly ferromagnetic antiferromagnet (NiF_2). Table I gives the known data regarding the structures.

Using as examples the transitions ${}^3A_{2g} \rightarrow {}^1T_{2g}^a$ and ${}^3A_{2g} \rightarrow {}^3T_{1g}^b$ in the Ni^{2+} ion, for which very narrow absorption bands exist at low temperatures, we consider the possible enabling mechanisms for these transitions in the investigated crystals. The narrowest absorption bands in RbNiF_3 , K_2NiF_4 , and NiF_2 were investigated with regard to their spectral positions and widths in the temperature interval $1.3^\circ - 77^\circ\text{K}$.

The measurement technique has been described in^[3]. The samples were placed in a cryostat having transparent quartz windows. The absorption spectra were photographed with a DFS-8 diffraction spectrograph having 3 \AA/mm linear dispersion. The photometric work was then performed with an MF-2 microphotometer.

STRUCTURE OF THE ABSORPTION SPECTRA

Figures 1 and 2 show the absorption spectra of the given crystals for the transitions ${}^3A_{2g} \rightarrow {}^1T_{2g}^a$ and ${}^3A_{2g} \rightarrow {}^3T_{1g}^b$. Both transitions are symmetry-forbidden; the first transition is also spin forbidden, which may account for the fact that it is less intense than the other. It should first be noted that at low temperatures ($T < 77^\circ\text{K}$) these transitions in all the crystals consist of wide absorption bands with a distinct fine structure at the long wavelength edge. The details of the structure differ for the same transition in the different crystals.

In^[11] the fine structures of the two transitions in KNiF_3 have been interpreted as vibronic, with vibrational frequencies close to those found in the infrared spectrum.^[12,13]

We know that the electron-phonon interaction gives rise to vibronic sidebands in the light absorption spectrum; in the case of a strong interaction these satellites merge to form a broad quasi-continuous spectrum. In the case of antiferromagnetic crystals we can assume that the phonon mechanism is accompanied by a magnonic enabling mechanism;^[14] the ionic transition to an excited state is then accompanied by the generation of a spin wave. An analysis of the ${}^3A_{2g} \rightarrow {}^1T_{2g}^a$ transition in NiF_2 ^[15] has shown that the $\nu = 20\,622\text{ cm}^{-1}$ band (Fig. 1) can be associated with an electric-dipole transition that is allowed because of the interaction with a magnon of the maximum frequency $\nu_M = g\mu_B H_E = 100\text{ cm}^{-1}$ (H_E is the exchange field). The $\nu = 20\,717\text{ cm}^{-1}$ band results from the creation of an exciton and two magnons having equal but opposite momenta. The remaining bands of this transition can be accounted for within the framework of the usual vibronic mechanism participated in by known optical frequencies of the NiF_2 vibrational spectrum.

The structure of the RbNiF_3 and K_2NiF_4 spectra (Fig. 2) differs from that already considered for NiF_2 and KNiF_3 . In the case of the ${}^3A_{2g} \rightarrow {}^3T_{1g}^b$ transition single intense narrow band is observed, while the

Table I. Crystallographic and magnetic properties of the crystals

Compound	Lattice	Lattice parameter, Å	Magnetic structure	Magnetic ordering temperature, °K
RbNiF ₃	Hexagonal, BaTiO ₃ type $D_{6h}^4 - P6_3/mmc$ [7]	$a = 5.84$, $c = 14.31$ [7]	Ferroxyplan-type ferrimagnetic	$T_c = 145$ [9]
KNiF ₃	Cubic perovskite ная O_h^1 [7]	$a = 4.01$ [7]	Collinear antiferromagnetic	$T_N = 275$ [7]
K ₂ NiF ₄	Tetragonal	D_{4h}^{17} [7] $a = b = 4.006$, $c = 13.076$ [7]	Weakly ferromagnetic antiferromagnetic	$T_N = 225$ [7]
NiF ₂	Tetragonal	D_{4h}^{14} [8] $a = b = 4.71$, $c = 3.11$ [8]	Collinear antiferromagnetic	$T_N = 73.2$ [10]

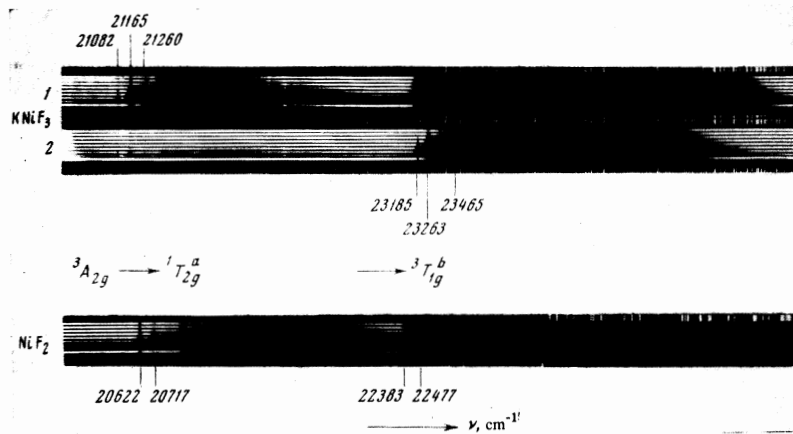


FIG. 1. Absorption spectra in the region of the transitions ${}^3A_{2g} \rightarrow {}^1T_{2g}^a$ and ${}^3A_{2g} \rightarrow {}^3T_{1g}^b$ for KNiF₃ crystals: 1— d (crystal thickness) = 1.8 mm, 2— d = 0.27 mm, and a NiF₂ crystal: d = 0.9 mm; T = 4.2°K.

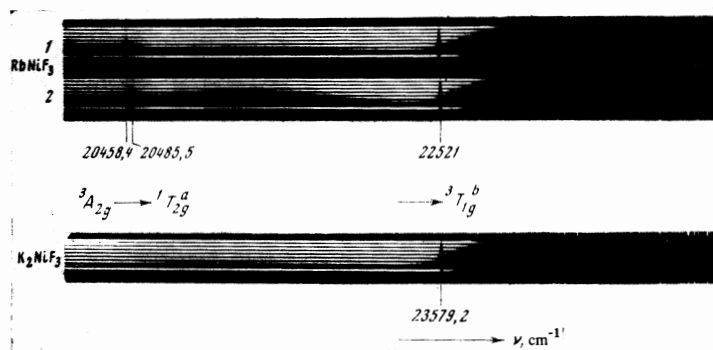


FIG. 2. Absorption spectra in the region of the transitions ${}^3A_{2g} \rightarrow {}^1T_{2g}^a$ and ${}^3A_{2g} \rightarrow {}^3T_{1g}^b$ for a RbNiF₃ crystal (d = 0.3 mm): 1— $E||C$, 2— $E \perp C$ (E is the electric vector of the light wave and C is the hexagonal axis of the crystal), and a K₂NiF₄ crystal (d = 0.8 mm); T = 4.2°K.

${}^3A_{2g} \rightarrow {}^1T_{2g}^a$ transition in RbNiF₃ is a doublet of such bands. Since the RbNiF₃ and K₂NiF₄ spectra did not reveal a clear vibrational structure and we have no data regarding vibrational infrared frequencies for these crystals, a vibrational analysis would be difficult. However, neither the shape nor the temperature dependence of frequencies in the given bands suggests that the mechanism enabling these transitions in RbNiF₃ and K₂NiF₄ is associated with the excitation of a spin wave; an electron-phonon mechanism appears to be more likely. A spin-orbit interaction can hardly lead to the observed fine structure at low temperatures for ${}^3A_{2g} \rightarrow {}^1T_{2g}^a$ especially, because of zero spin in the excited state. This mechanism can be excluded if we consider the similar structures of ${}^3A_{2g} \rightarrow {}^1T_{2g}^a$ and ${}^3A_{2g} \rightarrow {}^3T_{1g}^b$ in KNiF₃ and NiF₂. For RbNiF₃ and K₂NiF₄ the transition ${}^3A_{2g} \rightarrow {}^3T_{1g}^b$ consists of one intense

band (Fig. 2), whereas spin-orbit splitting should result in four bands.

Among the narrow bands comprising the fine structure of an identical electronic transition in Ni²⁺ as a component of crystals having different crystallographic and magnetic structures we therefore observe both electron-phonon and electron-magnon bands. We are thus able to compare the temperature dependences of the shapes and frequencies exhibited by bands resulting from these two different light absorption mechanisms.

TEMPERATURE DEPENDENCES OF ABSORPTION BAND SHAPES AND FREQUENCIES

For a detailed study of the temperature dependences of frequencies and shapes we selected the narrowest and most intense absorption bands in the spectra of our

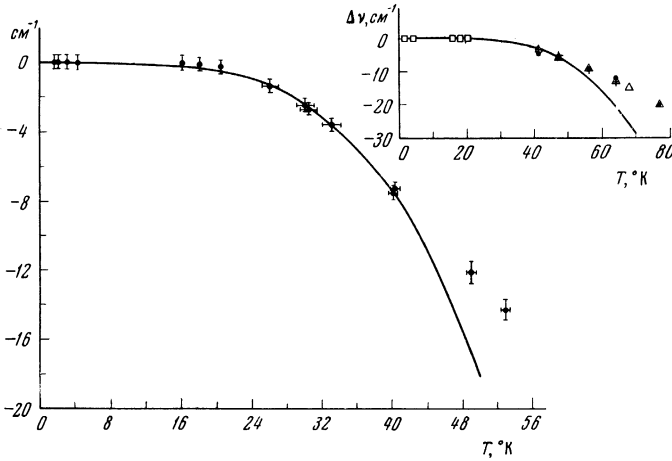


FIG. 3. Temperature dependence of the absorption-band-maximum frequency shift for RbNiF₃ (upper figure): ●- $\nu_0 = 20\,459\text{ cm}^{-1}$, +- $\nu_0 = 20\,485.5\text{ cm}^{-1}$, $\Delta-\nu_0 = 22\,521\text{ cm}^{-1}$; and for K₂NiF₄ (lower figure): ●- $\nu_0 = 23\,579.2\text{ cm}^{-1}$. In the range $T = 1.3^\circ\text{--}20^\circ\text{K}$ there is no shift; the points for all RbNiF₃ bands coincide at a given temperature and are designated by the symbol \square . The continuous theoretical curve was calculated from Eq. (1) with $l = 4$.

crystals: three bands of RbNiF₃ (the transitions ${}^3A_{2g} \rightarrow {}^1T_{2g}^a$ and ${}^3A_{2g} \rightarrow {}^3T_{1g}^b$), one band of K₂NiF₄ (${}^3A_{2g} \rightarrow {}^3T_{1g}^b$), and the $\nu = 20\,662\text{ cm}^{-1}$ band (${}^3A_{2g} \rightarrow {}^1T_{2g}^b$) of NiF₂. We thus investigated four electron-phonon (no-magnon) bands (for RbNiF₃ and K₂NiF₄) and one electron-magnon band (for NiF₂).

Figures 3 and 4 show the temperature dependences of the frequency shift $\Delta\nu = \nu_T - \nu_0$ and broadening $\Delta\delta = \delta_T - \delta_0$ exhibited by the investigated no-magnon absorption bands (ν_T and δ_T are the band frequency and half-width at the temperature T ; similarly, ν_0 and δ_0 at 0°K , or more accurately at 1.3°K (Table II). The frequencies were determined to within $\pm 0.2\text{ cm}^{-1}$, and the half-widths to within $\pm 0.6\text{ cm}^{-1}$.

All the investigated no-magnon bands can be approximated by asymmetric Lorentz curves having more highly developed short-wave wings (positive asymmetry sign in Table II). With increasing temperature the no-magnon band asymmetry diminishes for all our crystals. For $T > 20^\circ\text{K}$ they can be described, within error limits, by symmetric Lorentz curves.

In the entire investigated temperature region both the frequency shifts and the half-width changes for all bands of a single crystal can be described by identical equations:^[16]

$$\nu_T = \nu_0 - aT^l, \quad (1)$$

$$\delta_T = \delta_0 - bT^n. \quad (2)$$

FIG. 4. Temperature dependence of absorption band broadening for RbNiF₃: ●- $\nu_0 = 20\,458.4\text{ cm}^{-1}$, +- $\nu_0 = 20\,485.5\text{ cm}^{-1}$, $\Delta-\nu_0 = 22\,521\text{ cm}^{-1}$; and for K₂NiF₄: ○- $\nu_0 = 23\,579.2\text{ cm}^{-1}$. In the interval $T = 1.3^\circ\text{--}20^\circ\text{K}$ the bands are not broadened; the points for all bands coincide at a given temperature and are designated by the symbol \square . The continuous theoretical curves were calculated from Eq. (2) with $n = 4$.

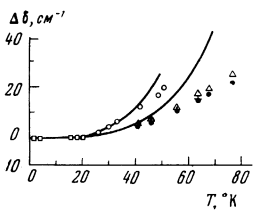


Table II. Characteristics of the optical bands

Compound	Transition	ν_0, cm^{-1}	δ_0, cm^{-1}	$a \times 10^6$ (cm^{-1})deg ⁴	$b \times 10^6$ (cm^{-1})deg ⁴	α
RbNiF ₃	${}^3A_{2g} \rightarrow {}^1T_{2g}^a$	20458.4	10	1.2	1.7	0.1
	${}^3A_{2g} \rightarrow {}^3T_{1g}^b$	20485.5	12.5	1.2	1.7	0.16
	${}^3A_{2g} \rightarrow {}^3T_{1g}^b$	22521	25	1.2	1.7	0.16
K ₂ NiF ₄	${}^3A_{2g} \rightarrow {}^3T_{1g}^b$	23579.2	15.5	2.9	4.1	0.06
NiF ₂	${}^3A_{2g} \rightarrow {}^1T_{2g}^b$	20622	12.3			-0.09

Remark: $\alpha = 2[(\nu_{\nu_0} - \nu_0) - (\nu_{\nu_0} - \nu_{\nu_0})]/\delta_0$ is the asymmetry of the band; $\nu_{\pm 1/2}$ are the frequencies at which K (the absorption coefficient) = $1/2 K_{\text{max}}$ on the short-wave (+) and long-wave (-) sides; $T = 1.3^\circ\text{K}$

The experimental data, recorded most carefully for K₂NiF₄, showed that the shifts of all the no-magnon absorption bands for $T \leq 40^\circ\text{K}$ are proportional to T^4 [$l = 4$ in Eq. (1), and the coefficient a varies from crystal to crystal]. The continuous theoretical curves in Fig. 3 represent (1); the values of a for the bands are given in Table II. With increasing temperature the frequency-shift curve becomes flatter, and becomes proportional to $T^{5/2}$ or T^3 within error limits. The result for $T \leq 40^\circ\text{K}$ agrees with theoretical calculations in^[6,16]. The constant a in (1) is of exchange character. From (1) we have

$$\nu_T - \nu_0 = aT^4 = M(T_N)(T/T_N)^4, \quad (3)$$

where $M(T_N) = aT_N^4 \approx 7330\text{ cm}^{-1} = 0.9\text{ eV}$ for K₂NiF₄ (Tables I and II). Using the approximation of^[6] we obtain

$$M(T_N) \approx T_N^4 / \Theta_N^3 \approx T_N(T_N / \Theta_N)^3, \quad (4)$$

whence we derive the exchange constant $\Theta_N \approx 5.5 \times 10^{-3}\text{ eV}$, agreeing in order of magnitude with the exchange integral estimates in^[17]. The observed agreement between experiment and theory can be regarded as a proof that it is correct to assume a relation between the actual shifts of antiferromagnet absorption bands and a spin-orbit exchange interaction.^[6]

The band-broadening measurements were subject to large errors. It is therefore more difficult at low temperatures to determine the exponent in (2) uniquely. It can be stated that n lies between $5/2$ and 4. However the linear relation between the frequency shift and broadening in the entire investigated temperature range for all the no-magnon absorption bands (Fig. 5) suggests that the shift and the broadening obey the same law ($l = n$). This experimental result also agrees with the theory in^[16]. Table II gives the coefficients a and b in (1) and (2) for all the bands with $n = l = 4$ when $T \leq 40^\circ\text{K}$.

It should be noted that good agreement with the theory in^[6,16] cannot be expected to occur over the entire temperature range; the theory was derived rigorously only for very low temperatures ($T \leq 0.1 T_N$), where the spin-wave approximation is applicable. Since the observed experimental broadening and shift data pertain to higher temperatures ($T \leq 0.6 T_N$), their interpretation would require taking into account the temperature dependence of the parameters characterizing the spin system (the exchange interaction field $H_E(T)$ and the magnetic anisotropy field $H_A(T)$).

Unlike the aforementioned no-magnon bands, the electron-magnon band $\nu = 20\,622\text{ cm}^{-1}$ of NiF₂ has

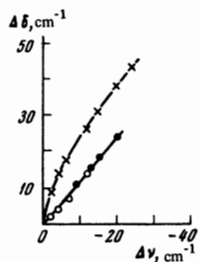


FIG. 5. Broadening of absorption bands versus shift for crystals of RbNiF_3 (●), K_2NiF_4 (○), and NiF_2 (+); $\nu = 20\,622\text{ cm}^{-1}$.

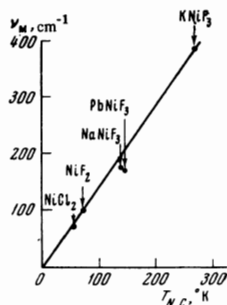


FIG. 6. Dependence of maximum magnon frequency on Neel temperature for crystals containing the nickel ion, according to different authors: for KNiF_3 ,^[18] RbNiF_3 and NaNiF_3 ,^[19] NiF_2 ,^[15] and NiCl_2 (private communication from Prikhot'ko and Ptukha).

negative asymmetry; its long-wavelength wing is therefore more highly developed (Table II). With a rise of temperature from 4.2° to 46°K (the region where this band exists) the asymmetry increases from -0.09 to -0.24 in accordance with Fig. 2 of^[15]. The broadening and shift for this band obey different laws; this results in a nonlinear relation between $\Delta\delta$ and $\Delta\nu$ (Fig. 5). The curve in Fig. 5 was plotted from the results presented in^[15]; the difference between the two curves furnishes an additional proof that the given band of NiF_2 is of magnonic origin. It should also be noted that the interval $\nu_M = 100\text{ cm}^{-1}$ observed in^[15] and interpreted as the maximum magnon frequency fits well on the straight line representing the dependence of the magnon frequency ν_M on the Néel temperature as plotted from the available experimental data for antiferromagnetic compounds containing Ni^{2+} (Fig. 6).

In conclusion, we wish to thank V. A. Popov for discussions of the results and for useful suggestions; also V. I. Silaev and N. V. Gapon for assistance with the measurements.

¹J. W. Stout, *J. Chem. Phys.* **31**, 709 (1959).

²S. Sugano and Y. Tanabe, Technical Report of ISSP, Japan, Series A, No. 71 (1963).

³V. V. Eremenko and A. I. Belyaeva, *Fiz. Tverd. Tela* **5**, 2877 (1963); **6**, 1967 and 3646 (1964) [*Sov. Phys.-Solid State* **5**, 2106 (1964); **6**, 1553 (1964) and 2918 (1965)].

⁴A. I. Belyaeva and V. V. Eremenko, *Zh. Eksp. Teor. Fiz.* **44**, 469 (1963) and **46**, 488 (1964) [*Sov. Phys.-JETP* **17**, 319 (1963) and **19**, 330 (1966)].

⁵M. A. Krivoglaz and G. F. Levenson, *Fiz. Tverd. Tela* **9**, 457 (1967) [*Sov. Phys.-Solid State* **9**, 349 (1967)].

⁶V. A. Popov, *Izv. Acad. Nauk SSSR, ser. fiz.* **30**, 927 (1966) [*Bull. Acad. Sci., Phys. Ser.* **30**, 968 (1966)]; *Fiz. Tverd. Tela* **8**, 3339 (1966) [*Sov. Phys.-Solid State* **8**, 2666 (1967)].

⁷W. von Rüdorff, J. Kändler, and D. Babel, *Z. anorg. Chemie* **317**, 261 (1962).

⁸B. F. Ormont, *Struktury neorganicheskikh veshchestv* (Structures of Inorganic Substances), Gostekhizdat, 1950.

⁹G. A. Smolenskiĭ, V. M. Yudin, P. P. Syrnikov, and A. B. Sherman, *Fiz. Tverd. Tela* **8**, 2965 (1966) [*Sov. Phys.-Solid State* **8**, 2368 (1967)].

¹⁰J. W. Stout and E. Catalano, *Phys. Rev.* **92**, 1575 (1953).

¹¹J. Ferguson, H. J. Guggenheim, and D. L. Wood, *J. Chem. Phys.* **40**, 822 (1964).

¹²A. Tsuchida and I. Nakagawa, *J. Phys. Soc. Japan* **20**, 1726 (1965).

¹³M. Balkanski, P. Moch, and M. K. Teng, *J. Chem. Phys.* **46**, 1621 (1967).

¹⁴R. L. Greene, D. D. Sell, W. M. Yen, A. L. Schawlow, and R. M. White, *Phys. Rev. Lett.* **15**, 656 (1965).

¹⁵A. I. Belyaeva, V. V. Eremenko, N. N. Mikhaĭlov, V. N. Pavlov, and S. V. Petrov, *Zh. Eksp. Teor. Fiz.* **50**, 1472 (1966) [*Sov. Phys.-JETP* **23**, 979 (1966)].

¹⁶V. A. Popov and A. A. Loginov, Report at 10th Intern. Conf. on Low Temperature Physics, Moscow, 1966.

¹⁷A. J. Freeman and R. E. Watson, *Phys. Rev.* **124**, 1439 (1961).

¹⁸K. Knox, R. G. Shulman, and S. Sugano, *Phys. Rev.* **130**, 512 (1963).

¹⁹N. N. Nesterova, I. G. Siniĭ, S. D. Prokhorova, and R. V. Pisarev, Report at All-Union Seminar on Magnetic Resonance and Spin Waves, Leningrad, 1967.

Translated by I. Emin